Overvoltages due to Single-Phase-to-Ground and Double-Phase Faults on a 20 kV Feeder

WALUYO[1], Siti SAODAH[2], Febriany Kalatiku SARANGA[1]

[1]Department of Electrical Engineering, Institut Teknologi Nasional Bandung (ITENAS), Jl. PHH. Mustafa No. 23, Bandung 40124, Indonesia.
[2]Department of Energy Conversion, Politeknik Negeri Bandung (POLBAN), Jl. Gegerkalong Hilir, Ciwaruga, Bandung Barat, 40559, Indonesia.

Abstract

One fault classification is an asymmetric fault, which causes a voltage and current on each phase to be unbalanced. This study analysed the voltage variations, including overvoltages, due to single-phase-to-ground and double-phase faults on a 20 kV three-phase distribution feeder. Both computations and simulations were carried out at 25%, 50%, 75%, and 100% of the feeder length, and further compared for analysis. From the comparison results, it was obtained that, as the point of fault far away, the source on the feeder, the fault currents would reduce, both for single-phase-to-ground and double-phase faults, both for simulation and computation. While, the healthy phase voltage, on the single-phase-to-ground fault, rose 1.61 up to 1.74 for the simulations and 3.46 up to 5.28 for the computations compared to the normal voltage. Finally, the faulty phase voltages, on the double phase-fault, reduced to 0.5 for the simulation and 0.45 up to 0.81 for the computation to the normal voltage.

Keywords: distribution feeder, double-phase fault, overvoltage, single-phase-to-ground fault, unbalanced

Received: 05 January 2020

To cite this article:
WALUYO, SAODAH S., SARANGA F.K., "Overvoltages due to Single-Phase-to-Ground and Double-Phase Faults on a 20 kV Feeder", in *Electrotehnica, Electronica, Automatica (EEA)*, 2020, vol. 68, no. 1, pp. 05-11, ISSN 1582-5175.

1. Introduction

Overvoltages take place both on power lines, including distribution feeders, and in transformers, including shunt reactors. The significant overvoltages are usually caused by lightning impulses and switchings [1-3]. Temporary overvoltages are also well known caused by phase-to-ground faults and neutral point shiftings [4-12]. Moreover, they are also caused by back-feeding on networks [13].

Some faults cause overvoltages and, concerning ground faults, arcing faults [14-15]. The probability of 0.05 is he phase-to-ground overvoltages that more than 2.3 times [16], and ground faults can be detected by zero-sequence voltage magnitude [17].

Transient overvoltages are also caused by single-phase-to-ground faults and substation breaker openings [18]. Distorted wave shape overvoltages are mainly caused by characteristics of transformer saturation [19], and the overvoltages are due to islanding and coordination with reclosing [20]. Resistive grounding applications of neutrals reduce overvoltages [21], and incipient faults also create considerable overvoltages [22].

Overvoltages are also caused by transformer back feed with a single-phase opening [23]. Asymmetrical lines are a destructive influence on phase angles [24]. A single phase-line-to ground fault condition is critical for some arc suppression method [25]. It is the most frequent fault in power distribution networks [26].

Arcing faults in an unearthed network can lead to overvoltages, more than double a phase-to-ground normal voltage [14].

Figure 1 shows a three-phase generator with $\mathbf{Z_f}$ grounded Impedance.

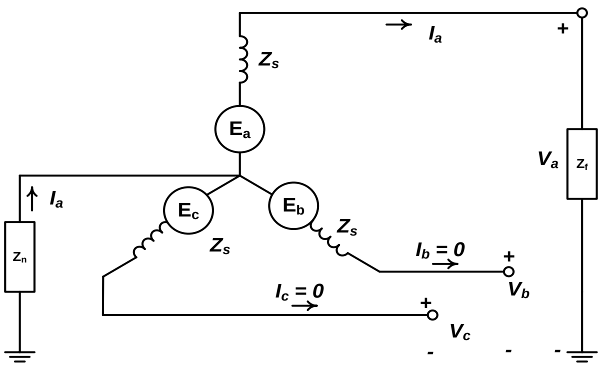

Figure 1. Generation phase to ground fault

where:

E_a, E_b, E_c are the three-phase generated voltages,
V_a, V_b, V_c are the voltages at the generator terminal,
I_a, I_b, I_c are the phase currents,
Zs is the generator impedance,
Z_f is the fault impedance to the ground.

The generator supplies a three-phase balanced load.

Using Kirchhoff's law on each phase, it can be obtained the following equation [27]:

$$V_{ag} = Z_f \, I_a \tag{1}$$

$$I_b = I_c = 0 \tag{2}$$

A substitution is made in the equation $I_b = I_c = 0$ to the symmetrical component of current equations [27].

$$\begin{bmatrix} I_0 \\ I_1 \\ I_2 \end{bmatrix} = \frac{1}{3} \begin{bmatrix} 1 & 1 & 1 \\ 1 & a & a^2 \\ 1 & a^2 & a \end{bmatrix} \begin{bmatrix} I_a \\ 0 \\ 0 \end{bmatrix} = \frac{1}{3} \begin{bmatrix} I_a \\ I_a \\ I_a \end{bmatrix} \tag{3}$$

$$I_0 = I_1 = I_2 = \frac{V_f}{Z_0 + Z_1 + Z_2 + 3Z_f} \tag{4}$$

$$I_a = I_0 + I_1 + I_2 = 3I_1 = \frac{3V_f}{Z_0 + Z_1 + Z_2 + 3Z_f} \tag{5}$$

$$\begin{bmatrix} V_0 \\ V_1 \\ V_2 \end{bmatrix} = \begin{bmatrix} 0 \\ V_f \\ 0 \end{bmatrix} - \begin{bmatrix} Z_0 & 0 & 0 \\ 0 & Z_1 & 0 \\ 0 & 0 & Z_2 \end{bmatrix} \begin{bmatrix} I_0 \\ I_1 \\ I_2 \end{bmatrix} \tag{6}$$

$$\begin{bmatrix} V_{ag} \\ V_{bg} \\ V_{bc} \end{bmatrix} = \begin{bmatrix} 1 & 1 & 1 \\ 1 & a^2 & a \\ 1 & a & a^2 \end{bmatrix} \begin{bmatrix} V_0 \\ V_1 \\ V_2 \end{bmatrix} \tag{7}$$

Figure 2 shows a double-phase fault on **b** and **c** phases through an impedance.

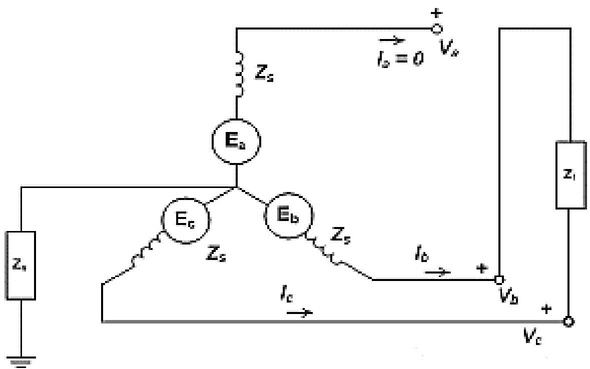

Figure 2. Double-phase fault

It is assumed that the generator is in a no-load condition, so that we can get the equations as below [27].

$$I_a = 0 \tag{8}$$

$$I_c = -I_b \tag{9}$$

$$\begin{bmatrix} I_0 \\ I_1 \\ I_2 \end{bmatrix} = \frac{1}{3} \begin{bmatrix} 1 & 1 & 1 \\ 1 & a & a^2 \\ 1 & a^2 & a \end{bmatrix} \begin{bmatrix} 0 \\ I_b \\ -I_b \end{bmatrix} = \begin{bmatrix} 0 \\ \frac{1}{3}\left(a - a^2\right) I_b \\ \frac{1}{3}\left(a^2 - a\right) I_b \end{bmatrix} \tag{10}$$

line-to-line fault conditions in sequence domain:

$$\begin{aligned} I_0 &= 0 \\ I_2 &= -I_1 \\ V_1 - V_2 &= Z_f \, I_1 \end{aligned} \tag{11}$$

$$V_b = V_c = Z_f \left(I_b + I_c\right) \tag{12}$$

$$I_a = I_a^0 = I_a^1 = I_a^2 = 0 \tag{13}$$

Based on this introduction and theory, it is necessary to investigate current and voltage variations due to single-phase-to-ground and double-phase (phase-to-phase) faults. Both parameters were carried out computations and simulations using software, 25%, 50%, 75%, and 100% feeder.

2. Materials and Methods

This research consisted of some stages, such as collecting required data of 20 kV distribution network.

The required data in this research were: single line diagram, cable type, the distance between line, line length, cable impedance, transformer nameplate, transformer capacity, and short circuit current. The data analysis also referred to the computational results with the simulation.

The impedances are three kinds of sequence impedances: positive, negative, and zero sequence impedances.

The source positive and negative sequence impedance is [27]:

$$Z_{S1} = Z_{S2} = \frac{(kV)^2}{MVA_{sc3\phi}} \tag{14}$$

The source zero sequence impedance:

$$Z_{S0} = \frac{(kV)^2}{MVA_{sc1\phi}} \tag{15}$$

Transformer positive and negative sequence impedances:

$$X_{t1} = X_{t2} = \frac{(kV)^2}{MVA} \, x \, Z_s \tag{16}$$

The power transformer that supplied CDM feeder had the connection of Y_{nyn0}, which had the star windings.

So, that reactance as [27]:

$$X_t = R_N \, x \, X_t \tag{17}$$

To find out the line positive and negative sequence impedances, it used the equations as:

$$Z_{L1} = Z_{L2} = n\% \, x \frac{(R_{L1} + j\, X_{L1})}{(\Omega / km)} x \, l(km) \tag{18}$$

To find out the line zero sequence impedance, it used the equations as:

$$Z_{L0} = n\% \, x \frac{(R_{L0} + jX_{L0})}{(\Omega / km)} x l(km) \tag{19}$$

The equivalent impedance was the summation of the transformer impedance (Z_t), system impedance (Z_s), and line impedance (Z_L). The positive and negative sequence impedance is:

$$Z_{1equiv} = Z_{2equiv} = Z = Z_t + Z_s + Z_L \tag{20}$$

$$Z_{0equiv} = Z = Z_t + Z_s + Z_L \tag{21}$$

In this study, it is revealed two fault conditions, single-phase to ground and double phase faults. The two-phase short circuit current of fault is [27]:

$$I_{sc} = \frac{V_f}{z_1 + z_2} \tag{22}$$

where V_f, Z_1, and Z_2 are the voltage at the fault point just before the fault, positive sequence impedance, and negative sequence impedance.

The single-phase to ground short-circuit fault current is [27:

$$I_{sc1\phi} = \frac{3V_f}{(z_0 + z_1 + z_2) + 3Z_f} \tag{23}$$

where Z_0 and Z_f are zero sequence and fault impedances, respectively.

The voltage variations in the event of single-phase to ground fault can be obtained by finding the zero, positive, and negative sequence voltages as [27]:

$$\begin{bmatrix} V_0 \\ V_1 \\ V_2 \end{bmatrix} = \begin{bmatrix} 0 \\ V_f \\ 0 \end{bmatrix} - \begin{bmatrix} Z_0 & 0 & 0 \\ 0 & Z_1 & 0 \\ 0 & 0 & Z_2 \end{bmatrix} \begin{bmatrix} I_0 \\ I_1 \\ I_2 \end{bmatrix} \tag{24}$$

where:

$$V_f = 3xV_{ph-n} \tag{25}$$

The computation of phase voltages is as follows:

$$\begin{bmatrix} V_{ag} \\ V_{bg} \\ V_{cg} \end{bmatrix} = \begin{bmatrix} 1 & 1 & 1 \\ 1 & a^2 & a \\ 1 & a & a^2 \end{bmatrix} \begin{bmatrix} V_0 \\ V_1 \\ V_2 \end{bmatrix} \tag{26}$$

The voltage variation in the event of double-phase fault can be obtained by finding the zero, positive, and negative sequence voltages as the following computations [27]:

$$\begin{bmatrix} V_0 \\ V_1 \\ V_2 \end{bmatrix} = \begin{bmatrix} 0 \\ V_f \\ 0 \end{bmatrix} - \begin{bmatrix} 0 & 0 & 0 \\ 0 & Z_1 & 0 \\ 0 & 0 & Z_2 \end{bmatrix} \begin{bmatrix} 0 \\ I_1 \\ -I_2 \end{bmatrix} \tag{27}$$

where:

$$V_f = 3xV_{ph-n} \tag{28}$$

The computation of the phase voltages at the time of the fault is as equation [26]. The notation of "**a**" in equations (26) and (28) is operator $1\angle 120^{o}$.

Figure 3 shows the single line diagram that made simulation using the software.

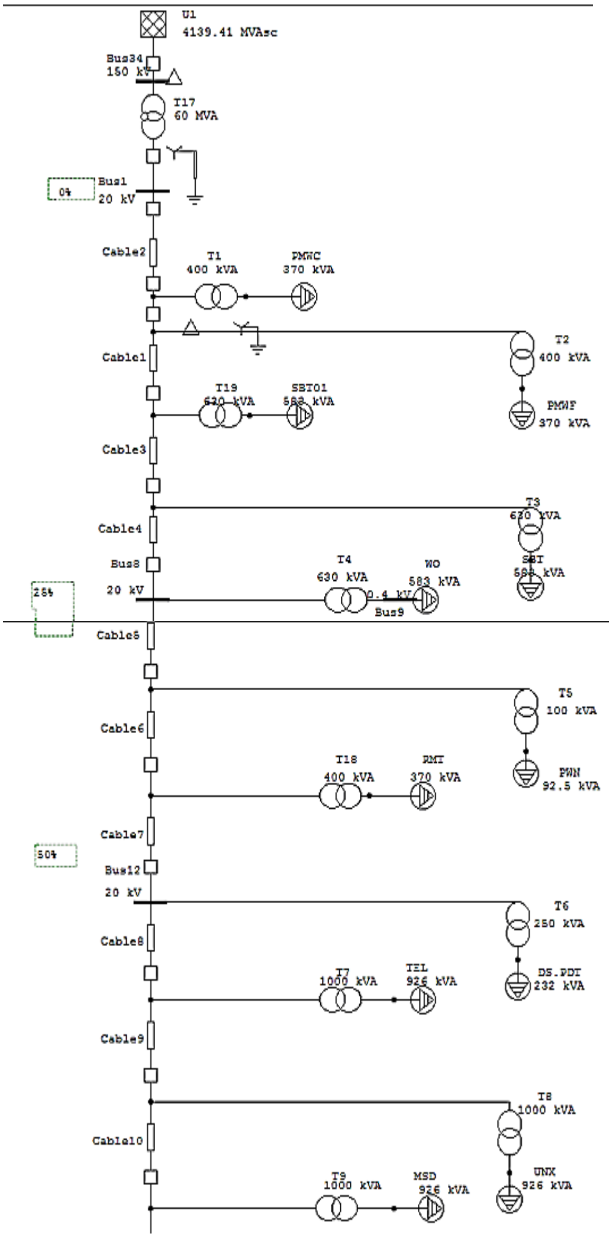

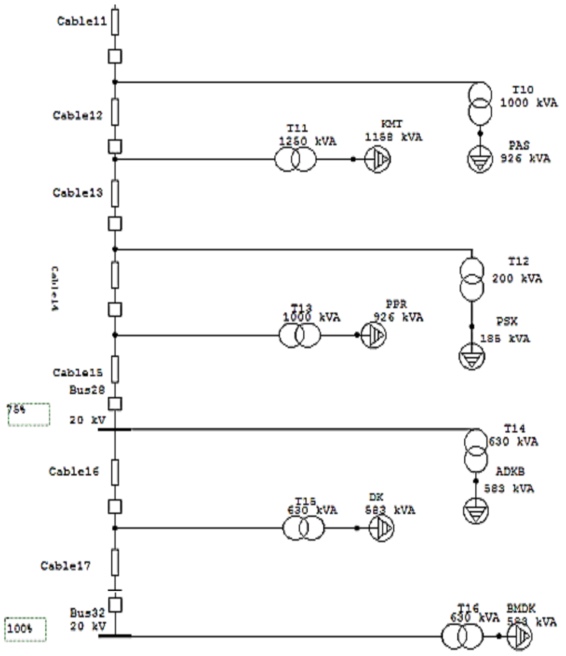

Figure 3. The simulated single line diagram

It represents a 20 kV feeder that supplies 18 distribution transformers to convert the secondary voltage of 400 V. It also uses power cables. The results of the simulation results would be compared to the computational ones.

3. Results and Discussion

The used sample network in the computations and the simulations, which caused voltage variations due to single-phase-to-ground and double-phase was CDM feeder of medium voltage 20 kV distribution network, using line cable.

Table 1 lists the cable data of CDM feeder, where the cable type was NA2XSEBY 3 x 240 and the resistance of 0.162 (Ω/km).

Table 1. Cable data of CDM feeder

No	Cable			Transformers	
	Initial	End	Length (km)	Name	Capacity (kVA)
1	E	PMWC	0.3120	PMWC	400
2	PMWF	SBT01	0.4870	PMWF	400
3	SBT01	SBT	0.6710	SBT01	630
4	SBT	WO	0.4430	SBT	630
5	WO	PWM	0.2290	WO	630
6	PWM	RMT	0.1580	RMT	400
7	RMT	DS.PDT	1.1230	PWN	100
8	DS.PDT	TEL	0.0780	DS.PDT	250
9	TEL	UNX	0.0320	TEL	1000
10	UNX	MSD	0.0320	UNX	1000
11	MSD	PAS	0.0430	MSD	1000
12	PAS	KMT	0.0820	PAS	1000
13	KMT	PSX	0.1290	KMT	1250
14	PSX	PPR	0.3860	PSX	200
15	PPR	BSH	0.4370	PPR	1000
16	BSH	ADKB	1.1830	ADKB	630
17	ADKB	DK	0.7620	DK	630
18	DK	BMDK	0.2400	BMDK	630

On the 20 kV conductor, the zero, positive, and negative sequence impedances were $0.277\angle 6.02°\Omega$, $0.158\angle 37.81°\Omega$, and $0.158\angle 37.81°\Omega$, respectively while the impedance of low voltage side of the power transformer is X_s=j0.096Ω.

Table 2 lists the transformer data to support the computations and simulations.

Table 2. Transformer data

Parameter	Quantity	Unit
Capacity	60	MVA
Frequency	50	Hz
Vector group	Yy	
Impedance (X_t)	14.13	%
High voltage	150	kV
Low voltage	20	kV
$I_{nominal}$ at 20kV	1732	A
Ground Resistance	12	Ω

Table 3 lists the positive, negative, and zero sequence impedances at 25%, 50%, 75%, and 100% of the feeder length.

Table 3. Positive, negative and zero sequence impedances

Distance (%)	Z_1 and Z_2 (Ω)	Z_0 (Ω)
25	0.213 + j0.166	0.47 + j0.05
50	0.427 + j0.331	0.94 + j0.1
75	0.640 + j0.497	1.41 + j0.15
100	0.853 + j0.663	1.88 + j0.2

The positive and negative sequence equivalent impedances are obtained from the sum of positive and negative source impedances, positive and negative sequence transformer impedances, and positive and negative feeder impedances.

Furthermore, to obtain the equivalence impedance of positive or negative sequence, it was used the formula as:

$$Z_{1quiv} = Z_{s1} + Z_{T1} + Z_{1\,feeder} \tag{29}$$

The equivalent impedances in the locations of the fault points were 25%, 50%, 75%, and 100%, as listed in Table 4.

Table 4. Equivalent impedances for Z_{1eq} and Z_{2eq}

Distance (%)	Z_{1eq} & Z_{2eq} (Ω)	
	R	X
25	0.213	j1.421
50	0.427	j1.586
75	0.64	1.752
100	0.853	j1.918

The zero sequence equivalent impedances were obtained from the sum of the zero-sequence transformer impedance, the source impedance, and the zero-sequence feeder impedance.

Based on the neutral grounding system, the zero sequence impedances of CDM feeder could be computed on the location fault points were 25%, 50%, 75%, and 100%, as listed in Table 5.

Table 5. Zero sequence equivalent impedances

Distance (%)	Z_{0equiv} (Ω)	
	R	X
25	36.47	j0.99
50	36.94	j1.04
75	37.41	j1.09
100	37.88	j1.14

A possibility of single-phase to ground fault is caused by inter-pole interruption of one distribution wire, touched by a high enough tree. The computation of this fault can be based on the length of the feeder. The points of faulted computation were 25%, 50%, 75%, and 100% feeder length.

Figure 4 shows the computation and simulation results on the single phase-to-ground fault currents.

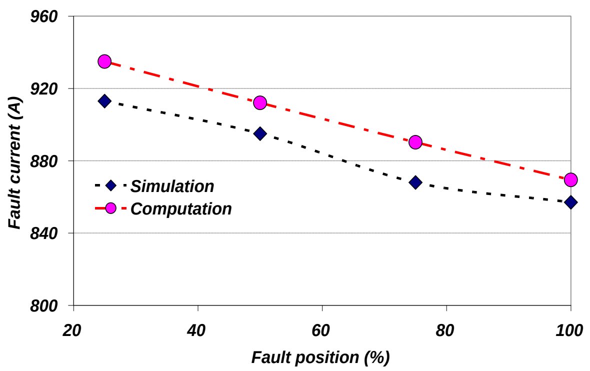

Figure 4. Comparative simulation and computation on the single-phase-to-ground fault currents

Based on the single-phase-to-ground computation, the fault current magnitudes are influenced by the distance of the fault points. The farther the distance of the fault point, the smaller the fault current, and vice versa, the closer the fault point, the higher the fault current. It tends to be hyperbolic chart forms.

This case is caused by the greater on the equivalent impedance. The fault current value would be smaller, and the closer the point of the location of the fault, the higher the fault current, due to the winding configuration of the power transformer affecting the fault resistance value.

The ratios of the fault currents between that at 100% and 25% feeder length are 0.930 and 0.939 for the computations, and the simulations respectively, or on average, the ratio is 0.934. While, the fault current ratios of the simulation and computational results are in the range 0.975 and 0.986, or the average is 0.980.

Therefore, the error for the comparison is 2.03%. It is relatively acceptable.

The computations of double-phase faults in this study were modelled the fault location point on 25%, 50%, 75%, and 100% distances.

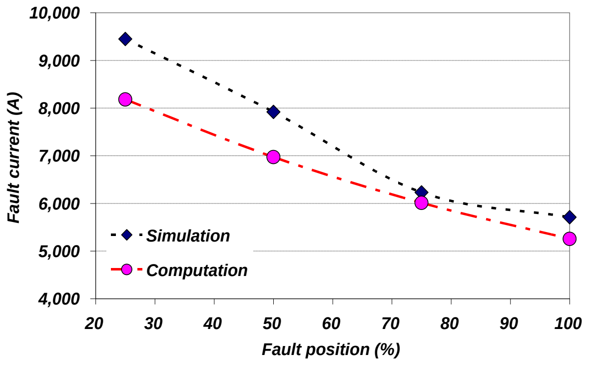

Figure 5. Simulation and computational double-phase fault current comparison

Based on Figure 5, the simulation double-phase fault currents were more significant than the computations. This case was probably caused by the cable impedance on the simulation had ideal value rather than on the computation where it used the cable impedance data from the site sample.

The ratios of the fault currents between that, at 100% and 25% feeder length, are 0.642 and 0.604 for the computations, and for the simulations respectively, or on average, the ratio is 0.623. While, the fault current ratios of the simulation and computational results are in the range 1.036 and 1.155, or the average is 1.103.

Therefore, the error for the comparison is -10.3%. It is relatively reasonable, although it is higher than that of the phase-to-ground fault.

Figure 6 shows the voltages in phase **b**, and **c** in the comparative simulation and computational results, about 60%, due to the value of the cable impedance in the computation followed the obtained data from the site, while the simulation using the software had the cable impedance based on the type of cable library.

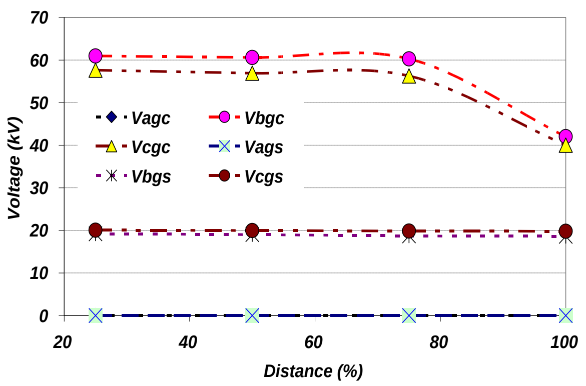

Figure 6. Comparative voltages due to single-phase-to-ground fault

Based on the figure, the voltage ratios in the **a** and **b** phases that did not experience any fault would increase.

This occurred was caused by the phase that has the fault (phase **a**) in the conductor to the ground where the voltage was very close to zero or become so low, so that there was an increase in voltage on the phase that was not disturbed (phase **b** and **c**).

The voltage variations in the event of a double-phase fault could be obtained by finding the zero, positive, and negative sequence voltages first. For the double-phase fault computation, it was modelled the location points of the fault at 25%, 50%, 75%, and 100% distances.

Figure 6 shows the voltages on phases **b** and **c** in the comparative simulation, and computational results increase at the point of review 25%-100% of the length of the feeder.

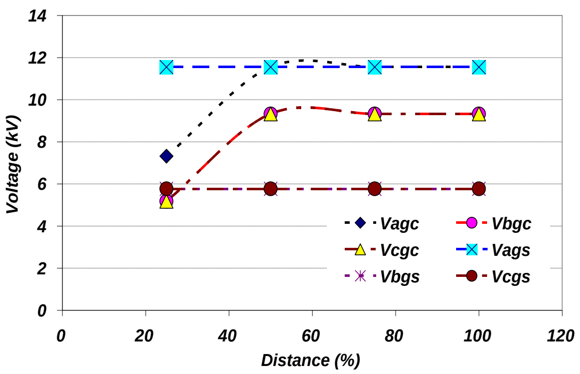

Figure 7. Comparative voltages due to double-phase fault

The average ratios of the overvoltages on phase **b** and **c** to the normal voltage are 4.847 and 4.564 for the computational results and 1.634 and 1.724 for the simulation results, respectively. It is clear that the phase-to-ground faults will elevate the healthy phase voltages. The differences in the values that occur between computational results and simulation results are probably caused by the cable impedance in the computation followed the obtained data from the site while in the simulation using the software, the cable impedance determination based on the cable library.

Based on the charts in Figure 7, the voltages on phase **b** and **c** in the comparative simulation and computational results decrease at the point of review 25%-100% of the length of the feeder.

The average ratios of the overvoltages on phase **b** and **c** to the normal voltage are 0.718 for the computational results and 0.500 for the simulation results, for both phases. It is clear that the phase-to-phase faults will decrease the faulty phase voltages.

The different values that occur between computational and simulation results are probably caused by the cable impedance in the computation followed the obtained data from the site while in the simulation using the software library.

4. Conclusions

Based on the type of the single-phase-to-ground faults, the fault currents decrease as the distance of fault location to the source increases, and both based the simulation and computational results. The charts tend to be hyperbolic forms. This case also applies to the double-phase faults. Nevertheless, the magnitudes are different from each other. The errors of the computation to the simulation are 2.03% and -10.3%, respectively. While on the single-phase-to-ground faults, the healthy phase voltages 4.847 and 4.564 based on the computational results, and 1.634 and 1.724 based on the simulation results, on average, times to the normal voltage, on phase b and c respectively. Nevertheless, on the double-phase faults, the faulty phase voltages reduce to 0.718 and 0.500, on average, to the normal voltage, based on the computational and simulation results, respectively.

5. Bibliographic References

[1] B. Jurišić, P. Poujade, A. Xemard, F. Paladian, Computation of internal overvoltages using a wideband transformer model based on limited information about transformer design, 4th International Colloquium Transformer Research and Asset Management, *Procedia Engineering*, 202 (2017), 288-296.

[2] B.F. Grčić, B. Franc, I. Uglešić, I. Pavić, S. Keitoue, I. Murat, I. Ivanković, Monitoring of transient overvoltages on the power transformers and shunt reactors – field experience in the Croatian power transmission system, 4th International Colloquium "Transformer Research and Asset Management," *Procedia Engineering*, 202 (2017) 29–42.

[3] M.A. Ravaglio, K.K. Küster, S.L.F. Santos, L.F.R.B. Toledo, A.P.A.E. Lazzaretti, L.G. de Mello, C.L. da S. Pinto, Evaluation of lightning-related faults that lead to distribution network outages: An experimental case study, *Electric Power Systems Research* 174 (2019) 105848.

[4] K.C. Bikić, M. Gazdović, F. Kelemen, A. Lojpur, Transferred Voltages due to Single Phase Earth Fault on Power Transformers, 4th International Colloquium Transformer Research and Asset Management, *Procedia Engineering* 202 (2017), 305-311.

[5] A. Cerretti, F.M. Gatta, A. Geri, S. Lauria, M. Maccioni, G. Valtorta, Temporary overvoltages due to ground faults in MV networks, *2009 IEEE Bucharest Power Tech Conference*, June 28th-July 2nd, Bucharest, Romania.

[6] A. Cerretti, F.M. Gatta, A. Geri, S. Lauria, M. Maccioni, G. Valtorta, Ground Fault Temporary Overvoltages in MV Networks: Evaluation and Experimental Tests, *IEEE Transactions on Power Delivery*, 27(3), July 2012, 1592-1600.

[7] S. Feng, L. Zheng, J. Lie, Y. Sun, G. Chen, X. Ji, Research on Arc-grounding Overvoltage in the 10kV Distribution System, 2012 International Conference on Future Energy, Environment, and Materials, *Energy Procedia* 16, 2012, 1785-1791.

[8] M. Ropp, A. Hoke, S. Chakraborty, D. Schutz, C. Mouw, A. Nelson, M. McCarty, T. Wang, A. Sorenson, Ground Fault Overvoltage With Inverter-Interfaced Distributed Energy Resources, *IEEE Transactions on Power Delivery*, 32(2), April 2017, 890-899.

[9] S. Ravlića, A. Marušićb, Simulation Models for Various Neutral Earthing Methods in Medium Voltage Systems, 25th DAAAM International Symposium on Intelligent Manufacturing and Automation, DAAAM 2014, *Procedia Engineering* 100 (2015) 1182-1191.

[10] C. Feltes, R. van de Sandt, F. Koch, F. Shewarega, I. Erlich, *2011 IEEE/PES Power Systems Conference and Exposition*, 20-23 March 2011, Phoenix, AZ, USA.

[11] S. Hänninen, *Single phase earth faults in high impedance grounded networks Characteristics,*

indication, and location, Dissertation for the degree of Doctor of Technology to be presented with due permission for public examination and debate in Auditorium S5 at Helsinki University of Technology (Espoo, Finland) on the 17th of December, 2001.

[12] R. Calone, A. Cerretti, F. M. Gatta, A. Geri, S. Lauria, M. Maccioni, G. Valtorta, Abnormal Ground Fault Overvoltages in MV Networks: Analyses and Experimental Tests, *International Conference on Electricity Distribution* Frankfurt, 6-9 June 2011, paper 0511.

[13] R. Salcedo, X. Ran, F. de León, D. Czarkowski, V. Spitsa, Long Duration Overvoltages due to Current Backfeeding in Secondary Networks, *IEEE Transaction on Power Delivery*, 28(4), Oct. 2013, 2500-2508.

[14] S. Hänninen, *Single phase earth faults in high impedance grounded networks, Characteristics, indication and location*, Dissertation for the degree of Doctor of Technology to be presented with due permission for public examination and debate in Auditorium S5 at Helsinki University of Technology (Espoo, Finland) on the 17th of December, 2001, at 12 o'clock noon, VTT Energy, VTT Publication 453, Technical Research Centre of Finland, ESPOO 2001.

[15] S. Ha¨nninen, M. Lehtonen, Characteristics of earth faults in electrical distribution networks with high impedance earthing, *Electric Power Systems Research* 44 (1998) 155-161.

[16] A. Yu. Vasilyeva, A. I. Shirkovets, A. V. Telegin, L. I. Sarin, M. V. Ilinykh, Transient Processes at Single Phase-to-ground Faults in Combined Grounded Networks, Proceedings of the *2011 3rd International Youth Conference on Energetics* (IYCE), 7-9 July 2011, IEEE, Leiria, Portugal.

[17] D. Flores, *Handling of Ground Fault in Distribution Networks, Regarding the Field Test Taken by SINTEF in 2005*, Master of Science in Energy and Environment, Norwegian University of Science and Technology, Department of Electric Power Engineering.

[18] C. Mozina, Impact of green power inverter-based distributed generation on distribution systems, *2014 67th Annual Conference for Protective Relay Engineers*, 31 March-3 April 2014, IEEE, College Station, TX, USA.

[19] H. B-L Lee, S.E. Chase, R.C. Dugan, Overvoltage Considerations for Interconnecting Dispersed Generators with Wye-Grounded Distribution Feeders, *IEEE Transaction on Power Apparatus and Systems*, Vol. PAS-103, No. 12, December 1984, 3587-3594.

[20] R. A. (Reigh) Walling, R. Saint, Roger C. Dugan, Jim Burke, Ljubomir A. Kojovic, Summary of Distributed Resources Impact on Power Delivery Systems Working Group on Distributed Generation Integration, *IEEE Transaction on Power Delivery*, Vol. 23, No. 3, July 2008, 1636-1643.

[21] K.P. Kadomskaja, A.V. Wishtibeev, On resistive grounding of the neutral in networks from 6 to 35 kV, Proceedings *Third Russian-Korean International Symposium on Science and Technology*. KORUS'99 (Cat. No.99EX362), 22-25 June 1999, IEEE, Novosibirsk, Russia, 738-740.

[22] [22] B. Kasztenny, I. Voloh, C.G. Jones, Detection of Incipient Faults in Underground Medium Voltage Cables, *2008 61st Annual Conference for Protective Relay Engineers*, 1-3 April 2008, IEEE, College Station, TX, USA

[23] D. Kunda, E. G. Neudorf, N. Perris, L.M. Szeto, D.V. Krause, Electrical impact of a NUG under 5 MW rating when connected to a distribution feeder with various transformer connections, Proceedings of *Industrial and Commercial Power Systems Conference*, 1-5 May 1994, IEEE, Irvine, CA, USA, USA.

[24] H. Li, J. Chen, Y. Liang, F. Liao, G. Wang, Effects of imbalance on single-phase to ground fault characteristics in low resistance grounded systems, *Electrical Power and Energy Systems* 115 (2020) 105504.

[25] J. Meng, W. Wang, X. Tang, X. Xu, Zero-sequence voltage trajectory analysis for unbalanced distribution networks on single-line-to-ground fault condition, *Electric Power Systems Research* 161 (2018) 17–25.

[26] X. Lin, S. Ke, Y. Gao, B. Wang, P. Liu, A selective single-phase-to-ground fault protection for neutral un-effectively grounded systems, *Electrical Power and Energy Systems* 33 (2011) 1012–1017.

[27] J.D. Glover, T.J. Overbye, M.S. Sarma, *Power System Analysis & Design*, Sixth Ed., 2017, Cengage Learning, pp.553-590.

Funding Sources

This work was technically supported by PLN Cigereleng Substation for providing the data.

Authors' Biographies

Waluyo was born in Magelang, Central Java (Indonesia), on January 2, 1969.
He graduated Institut Teknologi Bandung (ITB), Department of Electrical Engineering in Bandung (Indonesia), in 1994. He received the Master and Doctoral degrees in electrical engineering from the same university in 2002 and 2010, respectively.
Now, he works as an academic staff (associate professor) at the Department of Electrical Engineering, Institut Teknologi Nasional Bandung (Itenas). His research interests concern: high voltage engineering, transformer, and power system transmission.
e-mail: waluyo@itenas.ac.id

Siti Saodah was born in Cimahi, West Java (Indonesia), on November 27th, 1977.
She graduated Institut Teknologi Nasional Bandung (ITENAS), Department of Electrical Engineering in Bandung (Indonesia), in 2001. She received a Master's degree in electrical engineering from Institut Teknologi Bandung (ITB) in 2006.
Now, she works as an academic staff at the Department of Energy Conversion, Politeknik Negeri Bandung (Polban). Her research interests concern: high voltage engineering, transformer, and electric machines.
e-mail: siti@polban.ac.id

Febriany Kalatiku Saranga was born in Sorowako, Sulawesi (Indonesia), on February 02th 1993. She received B.Eng. Degree in electrical engineering from Institut Teknologi Nasional Bandung (Itenas), Indonesia, in 2018. Since 2018, she is a staff at a company.
Her research interests concern: electrical distribution system.
e-mail: febrianyksaranga@gmail.com